An article presented by Dr. Sibel Ügdüler and Prof. Steven De Meester *et al.* from Laboratory for Circular Process Engineering (LCPE), Department of Green Chemistry and Technology, Ghent University, Belgium.

Delamination and deinking of colored multilayer flexible plastic packaging *via* selective aminolysis of polyurethane and acrylate based adhesives

Selective aminolysis of polyurethane- and acrylate-based adhesives was developed as a single-step method for simultaneous delamination and deinking of multilayer flexible packaging. The effects of amine properties and film type on deinking efficiency were modeled quadratically. This selective aminolysis approach enabled recovery of intact polymer layers without dissolution or degradation, supporting their reuse in closed-loop recycling.

Image reproduced by permission of Pubrica - Scientific, Healthcare & Medical Research & Development from *Green Chem.*, 2025, **27**, 15485.

The cover artwork was created by Pubrica, Mr. Robert Ra (robert.ra@pubrica.com).

As featured in:

See Steven De Meester *et al.*, *Green Chem.*, 2025, **27**, 15485.

ROYAL SOCIETY OF CHEMISTRY

rsc.li/greenchem

Registered charity number: 207890

Green Chemistry

PAPER

View Article Online
View Journal | View Issue

Cite this: *Green Chem.*, 2025, **27**, 15485

Delamination and deinking of colored multilayer flexible plastic packaging *via* selective aminolysis of polyurethane and acrylate based adhesives

Sibel Ügdüler,[a] Tobias De Somer,[a] Noa Collier,[a,b] Martijn Roosen[a,c] and Steven De Meester*[a]

Received 28th May 2025,
Accepted 18th September 2025

DOI: 10.1039/d5gc02667a

rsc.li/greenchem

The demand for efficient recycling processes towards closed-loop recycling of multilayer plastic packaging is increasing. Delamination enables recovery of intact polymer layers without degrading main materials, offering economic and environmental benefits. Yet, scientific studies on the mechanisms of delaminating and deinking multilayer packaging remain limited despite strong industrial interest. This work presents key findings on the delamination and deinking mechanisms of multilayer flexible packaging films using selective aminolysis of the polyurethane and acrylate based adhesives. While aminolysis is widely used in plastic recycling, this study provides first insights into its targeted use for depolymerizing adhesives without affecting the main polymer layers. To investigate the relationship between specific amine properties and their effectiveness in deinking various types of plastic films including chemically stable UV-based inks, a quadratic model was developed. Among different properties, heat capacity, boiling point as proxy for polarity and molecular weight, dipole moment, and polar surface area emerged as key properties influencing deinking efficiency across different plastic films. The mechanism of selective aminolysis of the adhesive was investigated through FTIR and NMR analyses. Kinetic tests, based on a central composite inscribed (CCI) design, were conducted using a selected amine to assess the effect of process conditions for the colored PET/PE multilayer sample. The optimal conditions were identified as 65 °C, a particle size of 0.5 cm, and an S/L ratio of 0.01 g mL^{-1}. The impact of addition of chemical reagents on deinking and delamination efficiency was also explored, showing positive results depending on film composition.

Green foundation

1. This work presents a novel approach for the delamination and deinking of colored multilayer flexible plastic packaging, aiming to enhance closed-loop recycling and unlock both economic and environmental value of plastic waste.
2. This study provides first insights into selective aminolysis of polyurethane and acrylate based adhesives to recover constituent polymer layers of multilayer plastic packaging without any dissolution and degradation, paving the way for their reuse in closed-loop recycling.
3. The demonstrated single-step deinking and delamination process for a wide range of monolayer and multilayer plastic packaging is promising; however, future research should address solvent recovery and evaluate the environmental impact of the process to enable large-scale application.

1. Introduction

In order to advance towards a circular economy for plastics, policymakers are increasingly introducing regulations. For example, under the European Green Deal, the goal is to ensure that all plastic packaging placed on the EU market is recyclable in an economically viable manner by 2030, with an additional target for packaging to contain at least 30% recycled content.[1] The demand for high-quality recyclates thus becomes increasingly imperative considering that globally only 9% of plastic waste is recycled.[2] Together with ambitious goals set by policymakers industry engagement is crucial to reduce reliance on virgin resources, advancing circular products and services, and minimizing environmental impacts.[3–6] Chemical companies both within and outside the EU are taking important steps toward a more circular economy.[7–11] For instance, BASF has launched a new Circular Economy Program aimed at increasing the use of recycled and renewable feedstocks, establishing new material cycles, and developing innovative business

[a]*Laboratory for Circular Process Engineering (LCPE), Department of Green Chemistry and Technology, Ghent University, Graaf Karel De Goedelaan 5, 8500 Kortrijk, Belgium. E-mail: Steven.DeMeester@UGent.be*
[b]*Trevi nv-Gentbrugge Environmental Solutions, Dulle-Grietlaan 17/1, 9050 Gentbrugge, Belgium*
[c]*Catalisti vzw, Olieweg 95, 2020 Antwerp, Belgium*

models.[7] Similarly, Henkel has relaunched its bonding and sealing portfolio with a new packaging concept designed to increase the recycled content of packaging materials.[10] Such initiatives are crucial to improving closed-loop recycling rates. It is obvious that the composition of plastic packaging is a determining factor of the recycling efficiency. Especially for post-consumer flexible packaging, closed-loop recycling is still rare. Inks are essential for packaging but hinder recycling, often resulting in dark, low-quality recyclates. Residual inks can degrade during processing, causing odors and affecting material properties. Deinking is key to improving recyclate quality, but it's challenging due to the complex and varied ink compositions comprising solvents, resins, colorants, and additives. While nitrocellulose is common, more stable resins like PU, polyester, or PVB are preferred for high-temperature uses. UV-cured inks use reactive resins such as epoxy or urethane acrylates, and overprint varnishes further complicate removal.

Inks are essential for packaging but hinder recycling, often resulting in dark, low-quality recyclates. Residual inks can degrade during processing, causing odors and affecting material properties.[12,13] To improve recyclate quality and marketability, interest in deinking technologies is growing. However, ink removal remains challenging due to the complex composition of printing inks, which include solvents, resins, colorants, and additives.[14] Ink composition varies by application, substrate, and printing method. While nitrocellulose is common, more stable resins like PU, polyester, or PVB are preferred for high-temperature uses. UV-cured inks use reactive resins such as epoxy or urethane acrylates, and overprint varnishes further complicate removal.[15–17] Furthermore, for quite some packaging applications, the ink layer is embedded between polymer layers to prevent leaching.[18] To simultaneously improve barrier properties of a packaging, such different layers can consist of different polymer types which causes incompatibility issues in recycling. In this context, there is a significant drive to develop 'mono-material multilayers' which contain at least 80% of a single polymer *e.g.* polyethylene or polypropylene.[19] While these multilayer films align with current mechanical recycling objectives to avoid incompatibility between polymers, they still contain adhesives/tie layers and inks in the middle layers, which still results in dark colored and odorous plastic recyclates. Therefore, delamination and deinking of monomaterial multilayers is still needed to remove the inks and adhesives. This indicates that a combined deinking and delamination process can become a key technology to boost closed-loop recycling of both monolayer and mono/multi-material multilayer printed plastic films which are typically difficult to deink and delaminate due to their chemical resistance and limited solvent diffusivity *e.g.* UV-based printed plastic films and polyolefin based monomaterial multilayer plastic films.

Current mechanical recycling practices is based on different steps such as sorting, shredding, washing, density separation, drying and finally regranulation. The washing process then typically relies on cold or hot water, whether or not in presence of caustic soda and/or surfactants.[20] Some surfactants can also induce the removal of inks from plastic films.[21–25] Several initiatives already aim at commercialization of surfactant based deinking, such as the efforts by Keycycle, formerly called Cadel deinking.[26] Similarly, Sorema utilizes an advanced water-based washing system for the removal of inks.[27] Yet, a main drawback of surfactants is their limited effectiveness towards some ink structures *e.g.* UV-based crosslinked inks, and they are not able to penetrate into the polymer matrix, thus they are not always effective for removing inks from multilayer packaging.[28] Solvent-based purification (SBP) is also a widely used technique for recycling of plastic packaging.[29] In the context of deinking of plastic packaging, organic solvents were also widely studied for deinking of flexible plastic packaging. For example, the NorEC® process applies hot ethyl acetate to remove inks and some organic substances from polyolefins.[30] Similar to surfactants, ethyl acetate demonstrates limited effectiveness against crosslinked inks, especially when the ink layer is covered by polymer layers.[31,32] Alternatively, a polymer can be 'deinked' by dissolving the polymer in suited solvents, which allows to filter of the ink binder system which tends to stay solid.[33–38] This method has been applied in several industrial processes such as STAP, CreaSolv®, Newcycling®, and PureCycle.[39–42] However,[33–38] the effect of additives and inks on the purity of recovered polymers has hardly been considered in this process up to now. Furthermore, use of large solvent volumes increases the CAPEX of this technology, and it is a tedious process still facing processing problems such as high viscosity, gel formation and additive encapsulation.[43] Alternatively, delamination of multilayer structures by selective dissolution/depolymerization of the adhesive layer is a promising pathway for recycling of multilayer structures. This has been mainly applied on aluminum (Al) containing multilayers in acid media such as organic acids (*e.g.* acetic acid) or inorganic acids (*e.g.* nitric acid, phosphoric acid).[44–47] In general, only a few scientific papers have given attention to the mechanisms of delamination and deinking, studying for example the influence of different types of laminates such as covalent or hydrogen bonding between (corona treated) polymer layers and the adhesive *e.g.* polyurethane (PU) or acrylics.[48–51] These state-of-the art deinking and delamination processes are summarized in Table 1. Compared to current deinking and delamination methods, this study demonstrates a one-step process that can be applied to a wide range of monolayer and multilayer plastic packaging, including the removal of chemically resistant inks such as UV-cured inks.

In this study, selective aminolysis of adhesive and ink binders is proposed as a novel approach towards simultaneous deinking and delamination of monolayer and multilayer plastic films. To gain deeper insight in the mechanisms, a quadratic model is established that analyses the influence of amine properties and the type of plastic film on deinking efficiency for different plastic films. Furthermore, a specific case study is elaborated to analyse the delamination pathway of a printed multilayer film by focusing on the selective aminolysis of the PU adhesive. The parameters affecting the delamination and deinking process such as temperature, plastic flake size and solid/liquid ratio were assessed through a design of experiment.

Table 1 State-of-the-art deinking and delamination processes of plastic packaging

Medium type	Chemicals and conditions	Process	Applicable to	Limitations	Ref.
Aqueous medium	Water based alkaline medium w/ and w/o surfactants at *T* range between 50° and 100 °C	Deinking *via* solubilization of ink resin	Monolayer packaging	• Not effective on deinking and delamination of many multilayer packaging, including monomaterial multilayers • Generally slow process or ineffective on many binders, especially UV based inks	21–23 and 27
Inorganic acids	Conc./diluted inorganic acids *e.g.* nitric acid, sulfuric acid at moderate *T*	Delamination *via* degradation of adhesive/ polymer, deinking surface printed packaging	Polyolefin (PO) and Al based monolayer and multilayer packaging	• Harsh acidic conditions • Not applicable on PET • Limited delamination potential	46, 52 and 53
Organic acids	Conc/diluted organic acids *e.g.* formic acid, acetic acid w/ and w/o organic solvents at *T* range between 20° and 140 °C	Delamination *via* solubilization of adhesive	Mainly nonprinted PO and Al based multilayer packaging	• High operation *T* for high yield • Not effective for deinking	44, 45 and 47
Solvent-based medium – dissolution	Organic solvents *e.g.* toluene, DMSO at *T* above 80 °C	Delamination *via* selective dissolution-precipitation of polymer layers	Multilayer packaging, surface printed monolayer packaging	• Multiple process steps to recover each polymer • Need of high amount of antisolvent for polymer precipitation • Tedious process, beyond a 'wash'	42, 54 and 55
Solvent-based medium – chemical washing	Organic solvents *e.g.* ethyl acetate at *T* above 60 °C	Deinking *via* solubilization of ink resin	Monolayer packaging	• Limited delamination potential • Limited activity on many ink binder types • Not effective on removal of UV-based inks	30 and 56
Amine-based medium (this study)	Different types of amines w/ and w/o chemical reagents	Deinking and delamination *via* selective aminolysis of adhesive and ink binders	Broad range of colored monolayer and multilayer packaging including UV-based printed plastic packaging	• Need of safe handling • Potential odor issues at industrial level • Need of further research on solvent recovery and environmental assessment of the process due to potential ecotoxicity of the solvents	57

Furthermore, addition of chemical reagents alongside amines such as solvents to enhance polymer swelling and catalysts *e.g.* KOH to accelerate aminolysis was explored to further improve the efficiency of the delamination and deinking processes.

2. Materials and methods

2.1. Printed plastic films, chemicals, and reagents

Various types of monolayer and multilayer printed plastic films (Table 2) were used during selection of the potential amine. These plastic films were supplied by Siegwerk Druckfarben AG & Co. Films printed with UV-crosslinked acrylate is mainly used on rigid plastic packaging such as the labels of PET bottles and in-mold labeling.[58] Sample 4 containing low migration (LM) ink can be used in nutrition, pharma and hygiene (NPH) applications compared to sample 1, 2 and 3.[59] Samples 5, 6 and 7 are mainly used for food packaging.[60] Among these samples, samples 1 to 6 were used to screen various types of amines, whereas sample 7 was employed to assess the effect of deinking conditions through kinetic experiments. Following amines were used in the tests: ethylene diamine (Fluka Analytical ≥99.5%), 1-pentyl amine (Thermo scientific, 98%), dibutylamine (Merck, ≥99.5%), *N*-ethyl *N*-butyl amine (Merck, >98%), *N*-ethylcyclohexylamine (Alfa Aesar, 97%), diisopropylamine (Merck, >99%), tripropylamine (Merck, ≥98%), *N*,*N*-dimethylcyclohexylamine (Merck, 99%), 1,6 diamino hexane (Merck, 98%), dicyclohexylamine (Thermo

Table 2 Composition of monolayer and multilayer printed plastic films used in the tests

Sample number	Printing type	Layer 1	Layer 2	Layer 3	Layer 4	Layer 5
1	Acrylate, crosslinked	OPP, white	Cyan ink layer			
2	Acrylate, crosslinked	OPP, white	Cyan ink layer	Overprint varnish (OPV)		
3	Acrylate, crosslinked	OPP, transparent	White ink layer	OPP, transparent	Cyan ink layer	
4	Acrylate, crosslinked	OPP, transparent	White ink layer, low migration (LM) ink	OPP, transparent	Cyan ink layer, LM ink	
5	Solvent-free PU	OPP	NC-magenta	SF-PU adhesive	Transparent PE	
6	Solvent-free PU	PET	NC-black ink layer	PU-white ink layer	SF-PU adhesive	Alu-PP
7	Solvent-free PU	PET	NC-violet ink layer	PU-white ink layer	SF-PU adhesive	Transparent PE

scientific, 98%), *N*,*N*-dimethylbenzylamine (Merck, ≥99%), piperidine (Acros organics, 99%), triethylamine (Merck, ≥99.5%), and *N*,*N*-diethylcyclohexylamine (TCI, 98%).

To observe the impact of adding chemical reagents on the efficiency of deinking and delamination, the following chemicals were used in combination with *N*-ethyl *N*-butyl amine (EBA): ethanol (Merck, ≥99.5%), butanol (Merck, ≥99.4%), cyclohexane (Merck, ≥99%), and KOH pellets (Merck, >85%). During the tests, these chemicals were combined with EBA at varying volume ratios ranging from 25 v% to 75 v% at 60 °C for 4 hours. For KOH solution, a 1 w% KOH solution was prepared in water, and this solution was then mixed with EBA for the experiments. As a reference, the results obtained with EBA alone at 60 °C for 4 hours is given.

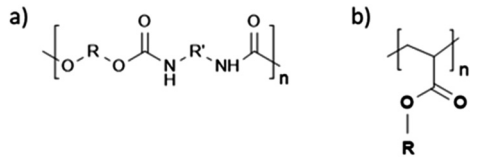

Fig. 1 (a) Polyurethane chemical structure; (b) acrylate chemical structure (used as crosslinked ink for samples 1, 2, 3 and 4).

The generic chemical structures of acrylate and PU compounds used in the inks of the tested samples are given in the figure below (Fig. 1).

2.2. Delamination and deinking experiments

Samples 1 to 6 (given in Table 2) were cut to a 1 cm × 1 cm flake size. Three pieces from each sample were then brought into contact with different amines at 75 °C for 4 hours. After testing a range of temperatures between 50 °C and 75 °C, it was observed that higher temperatures accelerated the deinking of plastic films. However, to remain below the boiling point of the amine and to prevent any risk of polymer dissolution, the operating temperature was set at 75 °C. In order to detect the effect of different primary, secondary and tertiary amines (given in Table 3) on the deinking and delamination rate of different samples, each 30 minutes the changes on the samples were noted. Deinking percentage of printed plastic films in different amines were determined through a reflection densitometry approach which detects the amount of residual pigment on the plastic film by means of the intensity of the reflected light. The collected plastic films from the liquid medium were rinsed with water, dried, and scanned together with two reference samples: one sample was a fully colored plastic film, and the other was an unprinted plastic film. A regular image scanner (Canon CanoScan LiDE 400) with a

Table 3 Amines and their corresponding properties used in the correlation matrix

Class	Amine	Boiling point (°C)	pK_b	Log *P* at 25 °C	MW (g mol^{-1})	Cp (J K^{-1} mol^{-1})	Dipole moment (D)	Dipole polarizability (× 10^{-24} cm^3)	Polar surface area (A^2)	Molar volume (cm^3 mol^{-1})
1° amine	1-Pentyl amine	104	3.40	2.9	87.2	120.2	0.12	0.31	26.0	91.9
1° diamine	Ethylene diamine	116	4.07	−2.0	60.1	78.2	0.19	0.14	52.0	60.8
	1,6 Diamino hexane	204.6	2.98	0.4	116.2	158.8	0.23	0.49	52.0	114.7
2° amine	Dibutyl amine	159	2.61	2.1	129.2	179.6	0.90	0.61	12.0	134.8
	N-Ethyl *N*-butyl amine	107.5	3.31	1.7	101.2	139.2	0.92	0.41	12.0	109.2
	N-Ethylcyclo hexyl amine	165	2.85	1.0	127.2	156.4	0.88	0.42	12.0	96.9
	Diisopropylamino	84	2.93	1.4	101.2	144.9	0.90	0.24	12.0	93.1
	Dicyclo hexylamine	255.8	3.60	2.7	181.3	214.4	0.88	0.64	12.0	158.2
	Piperidine	106	2.78	0.8	85.1	92.06	0.88	0.11	12.0	90.8
3° amine	Tripropylamine	156	3.35	2.5	143.3	202.3	0.33	0.32	3.2	132.2
	N,*N*-Dimethylcyclo hexylamine	158	3.28	2.3	127.2	157.1	0.53	0.34	3.2	125.6
	N,*N*-Dimethylbenzylamine	194	5.01	1.9	135.2	154.7	0.62	0.79	3.2	173.5
	Triethylamine	88.6	3.38	1.6	101.2	141.5	0.56	0.15	3.2	92.7
	N,*N*-Diethylcyclohexyl amine	193	3.31	2.7	155.3	198.5	0.57	0.47	3.2	174.3

resolution of 2550 × 3507 pixels was used for scanning. The settings (brightness: −40 units, contrast: +10 units) were to optimize visibility of transparent deinked samples. Subsequently, the images were processed using a program written in Python V3.9 programming language with the Open Source Computer Vision Library (OpenCV V4.5.5). The average deinking percentage of each sample in each medium was utilized to compare the effectiveness of the mediums. Detailed processing steps of determining ink density on the plastic films are given in Ügdüler *et al.*[32]

2.3. Construction of quadratic model to estimate deinking efficiency

To investigate the relationship between amine properties and their effect on the deinking efficiency of plastic films with different compositions, a quadratic model was constructed for each type of plastic film (samples 1–6) listed in Table 2. To achieve this, various properties of amines relevant to deinking and delamination were gathered through the COnductor-like Screening MOdel for Realistic Solvents (COSMO-RS) molecular modeling. The properties of amines considered consists of boiling point, pK_b value, log P value, molecular weight (MW), heat capacity, dipole moment, polar surface area, dipole polarizability and molar volume. To obtain these property values of different amines, COSMO-RS files were generated using Gaussian 16 and processed using Biovia Cosmotherm 20.0.0 (Dassault Systems). The properties of each amine gathered are in Table 3.

Afterwards, Pearson correlation coefficient matrix was examined to evaluate the correlation between the considered properties. The higher the absolute value, the stronger the correlation between the predictors. Therefore, predictors having coefficients with an absolute value higher than 0.7 were eliminated. The correlation matrix was created using the cor() function from the Stats package in R and is given in the SI, Fig. S1. Based on the correlation matrix, properties with high intercorrelation—such as volume, molecular weight (MW), dipole polarizability, and log P—were excluded from further analysis to avoid redundancy. In the construction of quadratic model, it was seen that pK_b value and molar volume were not significant, thus they are not included. A quadratic model with the adjusted R^2 value (0.71) was constructed for each plastic packaging based on the interaction of properties of boiling point, heat capacity, dipole moment and polar surface area. Residual analysis and Normal QQ plots given in Fig. S2 indicate that the identified outliers do not exhibit pronounced properties. Based on the significant amine properties, a quadratic model was constructed for each tested sample to estimate the deinking efficiency through following formula:

$$\%\text{Deinking}_{\text{sample}} = a \times X1 + b \times X2 + c \times X3 + d \times X4 + e \times X3^2 + f \times X4^2 \quad (1)$$

where, a, b, c, d, e, and f refer to the coefficients and $X1$, $X2$, $X3$, and $X4$ refer to the properties of boiling point, heat capacity, dipole moment and polar surface area, respectively.

2.4. Investigating the effect of process parameters and medium composition through kinetic tests

Additionally, kinetic studies were performed on the delamination and deinking of a violet colored PET/PE multilayer sample (sample 7 in Table 2) under different experimental conditions, as defined by central composite inscribed design (CCI). *N*-Ethyl *N*-butyl amine (EBA) was used as medium due to its high potential among the tested amines on this sample. The DoE was constructed based on three factors, namely temperature, particle size and solid/liquid (S/L) ratio as shown in Table 4. The limits of each factor were determined through exploratory experiments to adjust the parameters until a significant change in the delamination rate of MFPFs is observed. For example, while higher temperatures accelerate the deinking process of the plastic film, it was noted that the plastic film begins to curl at elevated temperatures, impeding effective delamination. Therefore, a maximum temperature of 65 °C was chosen for the kinetic studies. The S/L ratio was set between 0.01 g mL^{-1} and 0.05 g mL^{-1}, based on the maximum concentration of SF-PU adhesive reaction products (490 mg L^{-1}) observed after 2 hours of interaction with EBA at 65 °C. The particle size range was selected between 0.5 cm and 4 cm based on the standards typically used in the plastic cleaning industry.[61] The experiments for the kinetic study were carried out in a round-bottom flask equipped with a condenser and an overhead agitator with 2-blade impeller, operating at 300 rpm for consistent stirring. The 100 mL flask containing EBA was placed into a thermal bath at room temperature (RT) and preheated to the target temperature based on DoE prior to the addition of multilayer plastic film (sample 7) in order to minimize the delays prior to reaching the specified temperature at atmospheric pressure. During the 120 minutes of reaction, a 4 mL aliquot of liquid sample was collected from the medium

Table 4 Central composite inscribed experimental design (CCI) used to assess the effect of deinking and delamination conditions in *N*-ethyl *N*-butyl amine

Run	$X1$	$X2$	$X3$	T (°C)	T (K)	Size (cm)	SL (—)
1	−1	−1	−1	33	306.15	1.2	0.02
2	1	−1	−1	57	330.15	1.2	0.02
3	−1	1	−1	33	306.15	3.3	0.02
4	1	1	−1	57	330.15	3.3	0.02
5	−1	−1	1	33	306.15	1.2	0.04
6	1	−1	1	57	330.15	1.2	0.04
7	−1	1	1	33	306.15	3.3	0.04
8	1	1	1	57	330.15	3.3	0.04
9	−1.682	0	0	25	298.15	2.3	0.03
10	1.682	0	0	65	338.15	2.3	0.03
11	0	−1.682	0	45	318.15	0.5	0.03
12	0	1.682	0	45	318.15	4.0	0.03
13	0	0	−1.682	45	318.15	2.3	0.01
14	0	0	1.682	45	318.15	2.3	0.05
15	0	0	0	45	318.15	2.3	0.03
16	0	0	0	45	318.15	2.3	0.03
17	0	0	0	45	318.15	2.3	0.03
18	0	0	0	45	318.15	2.3	0.03
19	0	0	0	45	318.15	2.3	0.03
20	0	0	0	45	318.15	2.3	0.03

(50 mL) at every 30 minutes. The collected sample was subsequently transferred into a vial and immersed in an ice bath to stop further reaction of the polyurethane (PU) adhesive. These samples were then subjected to UV-VIS measurements. Utilizing calibration curves developed by using pure cured PU adhesive in EBA, the quantity of adhesive reaction products *e.g.* urea derivatives was quantified as explained in section 2.5.

The influence of process parameters were assessed through analysis of the kinetic experiment results. The delamination % in *N*-ethyl *N*-butyl amine (EBA) after 90 minutes of reaction time served as the reference point for comparing experimental conditions. The initial step involved analyzing the experimental datasets to identify outliers, achieved through residual plots generated by the plot function in R software. Subsequently, the resulting datasets were utilized to establish a quadratic model, describing the relationship between the experimental factors (temperature, S/L ratio, and particle size) and the delamination % after 90 minutes of interaction time. During the construction of the quadratic model, non-significant terms ($p > 0.05$) were incrementally removed, repeating this process until obtaining the quadratic model with the highest adjusted R^2. This iterative procedure was conducted using the Response Surface Methodology (RSM) package within the R environment. During the optimization, after excluding data points of experiment 2 as outliers, the adjusted R^2 value was 0.90, and the Lack of Fit (LOF) value was 0.11. The following equation was constructed to elucidate the effect of process parameters on the formation of reaction products:

$$Y = \beta_0 + \sum_{i=1}^{p} \beta_i X_i + \sum_{i=1}^{p} \sum_{j=1}^{p} \beta_{ij} X_i X_j + \sum_{i=1}^{p} \beta_{ii} X_i^2 \quad (2)$$

where Y is the response (delamination %), β_0 is the overall mean response, X_i and X_j refer to the i^{th} and j^{th} factor of the DoE, and β_i, β_{ij}, and β_{ii} refer to the coefficients describing the main effects for each factor, the two-way interaction between the i^{th} and j^{th} factors, and the quadratic effect for the i^{th} factor, respectively.

2.5. Analytical techniques for monitoring adhesive aminolysis

The medium containing the reacted PU adhesive and *N*-ethyl *N*-butyl amine (EBA) was analyzed *via* UV/Vis spectroscopy on a UV-1280 multipurpose UV/Vis spectrophotometer with a scan range of 190–1100 nm. The collected 4 mL aliquots were transferred into a semi-micro quartz cuvette with an outer cell dimension of 12.5 mm × 12.5 mm × 45 mm and an optical pathlength of 10 mm. Pure EBA solutions were measured as a reference. For each sample, the optical spectrum measurements were repeated three times to ensure their consistency and repeatability. In the spectrum, the strongest absorption was recorded at 280 nm for SF-PU adhesive reaction product. Based on the Beer–Lambert law [38], calibration curves were elaborated by using pure SF-PU adhesive at known concentrations. These curves were used to calculate the delamination percentage by correlating the concentration of reaction products with reaction time during the kinetic tests. During calculation of the amount of adhesive reacted in kinetic tests, a correction was made by considering the total amount of adhesive present in the reaction flask in the beginning of the experiment. This was performed by considering the density of the SF-PU adhesive (1.1 g cm^{-3}) and the mass of the SF-PU adhesive layer per cm^2 surface area of the violet colored PET/PE multilayer sample (sample 7) used in the kinetic tests (0.00033 g cm^{-2}). Afterwards, delamination % was expressed in terms of the mass of reacted adhesive which was calculated *via* the following equations:

$$M_A = \frac{M_{Total}}{M_{sample}} \times 0.00033\,(g\,cm^{-2}) \times A \quad (3)$$

$$\text{Delamination}\,(\%) = \frac{M_t}{M_A} \times 100 \quad (4)$$

where M_A is the total mass of adhesive present in the multilayer sample used in the kinetic test (g), M_{Total} is the total mass of multilayer sample used in the kinetic test (g), M_{sample} is the mass of one multilayer particle (g), A is the surface area of one multilayer particle (cm^2) and M_t is the mass of adhesive reacted in the solution medium at a specific time during kinetic studies (g).

In order to elucidate the mechanism of delamination and deinking, Fourier-Transform Infrared spectroscopy (FTIR) and proton nuclear magnetic resonance (NMR) measurements were performed on the EBA solution containing SF-PU adhesive. To achieve this, an excess amount of multilayer plastic films, sample 7, around 2 grams, was brought into contact with 20 mL of *N*-ethyl *N*-butyl amine (EBA) at 65 °C, the highest temperature utilized during the kinetic tests, for a duration of 2 hours. Afterwards, the solution was concentrated by using the rotavapor and the obtained crude product was collected for characterization. The FTIR measurements were recorded using the Omnic software in the range of 4000–400 cm^{-1}, at resolution of 4 cm^{-1} and with 32 scans. For each FTIR analysis, automatic smooth and baseline correction was applied. 1D proton NMR and 2D homonuclear COrrelation SpectroscopY (COSY) spectra (Fig. S3) were recorded using Bruker Avance 400 Ultrashield at room temperature in deuterated dimethyl sulfoxide (DMSO-d6). The spectra were analyzed using ACDLabs Spectrus Processor.

3. Results and discussion

3.1. Comparison of the effectiveness of different amines

To assess the impact of various amines on the deinking of different types of plastic films, six different plastic films given in Table 2 were tested in 14 different amines at 75 °C during 4 hours, after which a quantitative scan was taken on the deinked plastic film. Results are detailed in Table 5. Based on the experimental data, including replicates for each sample-amine combination, a two-factor ANOVA was conducted to assess the significance of differences among amines and film

samples. The ANOVA results showed highly significant effects, with p-values <0.05 for both amines and plastic film type. Moreover, the interaction between amines and samples was also significant ($p < 0.05$), indicating that deinking efficiency depends on both variables and their combined effects. To further identify specific differences between samples, paired t-tests were conducted, and the results are presented in Table S5. It is seen in the paired T-test that sample 1 is significantly different than other samples and shows the lowest deinking percentage across the different amines tested. Interestingly, despite the presence of an additional OPV layer in sample 2, its deinking percentage was higher compared to that of sample 1. This may be due to the OPV layer, which is typically applied as a protective coating over the ink layer. It helps to retain the ink within flakes, and during stirring, these flakes detach more easily, carrying unreacted PU with them. Regarding the multilayer samples (samples 3 to 6), deinking and delamination took longer due to curling of the samples. This occurs due to differences in the physical and chemical properties of the polymer layers, including mechanical stress, thermal expansion, and swelling behavior when exposed to liquid medium. Deinking of multilayer films with organic chemicals occurs in three stages.[48] First, there is a phase of liquid diffusion through the polymer layers. Second, the diffused molecules start reacting with the adhesive and ink binder. After complete reaction or dissolution, the deinking and delamination of the multilayer film is complete. As shown in Table S5, the p-values indicate that the deinking of sample 3 and 4 is significantly ($p < 0.05$) lower than the deinking efficiency of samples 5 and 6. Lower deinking performance of sample 3 and 4 could be due to the higher chemical resistance of UV-based inks and the presence of double ink layers, making the deinking process more challenging. This effect was more pronounced when in contact with secondary and tertiary amines, which have lower diffusivity through the polymer layers due to their larger molar volumes. Besides the number of ink layers, type of polymer used in the plastic film composition affects the diffusivity of the amine, thus affecting the deinking efficiency. For example, sample 5 (NC-magenta colored OPP/PE multilayer) containing a single ink layer exhibited for some amine types a lower deinking efficiency compared to sample 6 (NC-black colored PET/Al/PP multilayer) which contains a double ink layer, although overall among all amines, the difference is not significant based on the paired T-test (p value of 0.6). Since the type of amine significantly influences deinking efficiency (p-value of 2.06×10^{-90}), the observed difference in deinking performance between samples 5 and 6 is most likely attributed to variations in amine diffusivity through the distinct polymer structures of the two samples with some amines performing good on both samples and other (more polar ones) perform better on the PET containing samples.

Besides the plastic film composition, physicochemical properties of amines play a role in its capacity for deinking and delaminating plastic films. In order to investigate the relationship between the properties of the amines and their ability to deink different types of plastic films, the average deinking efficiencies of each sample in each amine given in Table 5 were used to establish a quadratic model for each sample.

$$\%\text{Deinking}_{\text{sample 1}} = 87.6 + 0.20 \times X1 + 2.2 \times X2 - 20.4 \times X3 + 85.1 \times X4 - 39.4 \times X3^2 - 42.8 \times X4^2 \quad (5)$$

$$\%\text{Deinking}_{\text{sample 2}} = 120.9 + 17.6 \times X1 - 9.2 \times X2 - 27.3 \times X3 + 67.1 \times X4 - 39.4 \times X3^2 - 42.8 \times X4^2 \quad (6)$$

$$\%\text{Deinking}_{\text{sample 3}} = 104.1 - 0.5 \times X1 + 0.5 \times X2 - 36.3 \times X3 + 106.2 \times X4 - 39.4 \times X3^2 - 42.8 \times X4^2 \quad (7)$$

Table 5 Average deinking % of 6 different plastic films given in Table 2 after in contact with 14 different amines at 75 °C for 4 hours. Standard deviation is given for the average deinking % of each sample in each amine

		Average deinking %					
Type	Amine tested	Sample 1	Sample 2	Sample 3	Sample 4	Sample 5	Sample 6
1° amine	1-Pentyl amine	14 ± 4.3	100 ± 0.0	100 ± 0.0	97 ± 1.1	100 ± 0.0	100 ± 0.0
1° diamine	Ethylene diamine	18 ± 3.7	12 ± 6.2	100 ± 0.0	96 ± 1.1	100 ± 0.0	100 ± 0.0
	1, 6 diamino hexane	21 ± 6.0	27 ± 1.3	100 ± 0.0	100 ± 0.0	100 ± 0.0	100 ± 0.0
2° amine	Dibutylamine	3 ± 2.7	8 ± 2.7	1.5 ± 1.8	2.5 ± 0.9	15 ± 9.8	83 ± 1.1
	N-Ethyl *N*-butyl amine	4 ± 1.4	6 ± 4.9	1.6 ± 2.8	2.7 ± 1.9	11 ± 9.9	70 ± 6.8
	N-Ethylcyclohexylamine	7 ± 3.5	100 ± 0.0	2.4 ± 2.6	98 ± 1.0	100 ± 0.0	100 ± 0.0
	Diisopropylamine	1 ± 0.4	0 ± 0.0	0.7 ± 1.2	1.4 ± 1.4	23 ± 6.5	62 ± 7.3
	Dicyclohexylamine	8 ± 8.6	100 ± 0.0	7.1 ± 4.8	1.0 ± 1.7	97 ± 5.1	68 ± 5.4
	Piperidine	8 ± 3.9	20 ± 11.9	1.7 ± 2.1	6 ± 5.6	100 ± 0.0	100 ± 0.0
3° amine	Tripropylamine	0 ± 0.0	0 ± 0.0	0 ± 0.0	0 ± 0.0	0 ± 0.0	15 ± 2.7
	N,*N*-Dimethylcyclohexylamine	6 ± 1.5	77 ± 6.5	0 ± 0.0	0 ± 0.0	72 ± 8.9	86 ± 6.8
	N,*N*-Dimethylbenzylamine	0 ± 0.0	18 ± 3.6	5.6 ± 7.9	7 ± 4.3	84 ± 6.4	79 ± 8.9
	Triethylamine	0 ± 0.0	60 ± 8.8	0 ± 0.0	0 ± 0.0	51 ± 10.9	15 ± 2.5
	N,*N*-Diethylcyclohexylamine	0 ± 0.0	29 ± 5.4	0 ± 0.0	0 ± 0.0	69 ± 6.8	12 ± 7.2

$$\%\text{Deinking}_{\text{sample 4}} = 110.7 + 3.7 \times X1 - 4.1 \times X2 - 28.0 \times X3 + 106.2 \times X4 - 39.4 \times X3^2 - 42.8 \times X4^2 \quad (8)$$

$$\%\text{Deinking}_{\text{sample 5}} = 147.1 + 41.1 \times X1 - 40.9 \times X2 - 26.9 \times X3 + 71.9 \times X4 - 39.4 \times X3^2 - 42.8 \times X4^2 \quad (9)$$

$$\%\text{Deinking}_{\text{sample 6}} = 151.9 + 17.7 \times X1 - 24.0 \times X2 - 9.1 \times X3 + 91.0 \times X4 - 39.4 \times X3^2 - 42.8 \times X4^2 \quad (10)$$

where, $X1$, $X2$, $X3$, and $X4$ refer to the properties of boiling point, heat capacity, dipole moment and polar surface area (PSA), respectively. The coded value of each property used to calculate the deinking efficiency based on the eqn (5)–(10) is given Table S3.

The generated quadratic equations were applied to validate the experimental results presented in Table 5. A consistent trend was observed between the model predictions and experimental deinking efficiency results for the various plastic films tested with different amines. For instance, *N*,*N*-diethylcyclohexylamine experimentally exhibited no deinking on samples 1, 3, and 4, while achieving the highest deinking efficiency on sample 5, followed by samples 2 and 6. The same deinking efficiency order was observed in the model predictions. The mean absolute error (MAE) between the modeled and experimental results, considering all tested samples and amines, was calculated to be 11.4%. The calculated deinking % values based on the quadratic equations and the calculation of the MAE are given in Table S4.

Based on these quadratic equations, the coefficients for boiling point and heat capacity of the amines are lower than those for dipole moment and polar surface area (PSA), indicating that their influence on deinking efficiency is less significant. In general, the positive coefficient of boiling point ($X1$) in the quadratic models indicates that amines with higher boiling points are associated with increased deinking efficiency. This is somehow a strange result, but is potentially linked to the specific structure of the amines in scope. Indeed, increased boiling point in our amine series is mainly caused by increase in alkyl chain length within the same class of amines which thus results in increasing apolarity of the amines enhancing diffusion through the apolar structure of polyolefins. Notably, sample 5 (NC-magenta colored OPP/PE multilayer) showed a stronger correlation with boiling point (coefficient value of 41.1 compared to other samples), likely because its double polyolefin layers. Similar to boiling point, heat capacity of amines also has small contribution on the deinking efficiency of samples. For most samples, the heat capacity coefficient in the quadratic models is negative, indicating that amines with higher heat capacities tend to exhibit lower deinking efficiency. Since solvents with higher heat capacity absorb more heat before experiencing a temperature increase, this may slow down the aminolysis reaction of inks and adhesives, especially due to the reaction's temperature-dependent rate. Exceptionally, sample 1 (monolayer OPP film with UV-based cyan ink) and sample 3 (OPP/OPP film with UV-based white and cyan ink) exhibited higher deinking efficiency with amines having a higher heat capacity. This could be attributed to the faster diffusion of amines, which facilitates deinking and delamination in these samples. Since these samples lack an OPV layer or low migration ink (LMI), the increased diffusion through the polyolefin layers in the presence of amines with higher heat capacity becomes a more determining factor for improving deinking efficiency compared to the aminolysis reaction itself. Among the various properties of amines, the dipole moment and polar surface area (PSA) showed the highest contribution to deinking efficiency. Since these two properties exhibit quadratic effects on deinking efficiency, their direct influence is not easily noticeable from the equation itself. Therefore, Fig. S4 illustrates the individual contribution of each amine property ($X1$, $X2$, $X3$, and $X4$) to the deinking percentage, providing a more intuitive visualization of their impact. As seen in Fig. S4, for all samples an inverse correlation between dipole moment and deinking efficiency was observed. Similar to the effect of heat capacity, a lower dipole moment indicates a smaller separation of charge or a more symmetrical electron distribution, which corresponds to decreased molecular polarity. This enhanced apolarity facilitates swelling of the apolar polymer matrix, such as polyolefins, allowing the amine to diffuse more effectively into the film and contribute to both delamination and deinking. As indicated by the equations, the quadratic coefficients of dipole moment and polar surface area (PSA) are the same for all samples, suggesting that their contributions to deinking efficiency are comparable. Based on the quadratic equations, It is seen that the deinking efficiency of the plastic films correlates directly with the PSA of the tested amines. It can be observed in Fig. S4 that PSA ($X4$) has quadratic impact on the response value for all the samples. Amines with higher PSA are able to interact more effectively with the polar adhesive and ink components, such as the polyurethane (PU)-based adhesive and nitrocellulose (NC)-based ink present in the tested samples. Despite the increased polarity of amines with higher PSA, amines like ethylene diamine, 1-pentyl amine, and 1,6-diaminohexane, which possess higher PSA, are primary amines, enabling them to diffuse more rapidly through the polymer layers. This combination of faster diffusion and stronger chemical interaction with adhesive and inks results in more efficient deinking and delamination of the plastic films. As shown, chemically resistant inks such as UV-based inks require harsher deinking conditions for effective removal. Therefore, developing new ink binders that incorporate reversible or cleavable bonds could enable easier removal of inks, including UV-based types, during recycling.[62–64]

3.2. Mechanism of delamination and deinking

To investigate the underlying mechanism of the delamination of multilayer samples, the reactivity of the PU adhesive was studied. For this, the multilayer structure laminated through

the aromatic polyester PU adhesive (sample 7, Table 2) was treated with *N*-ethyl *N*-butyl amine (EBA) at 65 °C for 2 hours. As shown in Fig. 2a, it is expected that the PU adhesive will undergo aminolysis during delamination with the amine, yielding urea and polyol adducts. Therefore, changes in the chemical structure of the PU adhesive were monitored using FTIR and NMR measurements (Fig. 2b and c, respectively). Detailed FTIR peaks of the pure cured SF-PU adhesive together with their description and assignment are given in the SI, Table S1.

The FTIR spectrum provides clear evidence of polyurethane undergoing aminolysis. Initially, the polyurethane spectrum displays characteristic peaks such as a broad N–H stretching (νN–H) band around 3320 cm^{-1}, a strong C═O stretching peak near 1700 cm^{-1}, and distinct C–N and C–O stretching vibrations at approximately 1220 cm^{-1} and 1000 cm^{-1}, respectively. Upon aminolysis, changes in the FTIR spectrum are observed. The N–H stretching peak shifted towards higher wavenumber (~3400 cm^{-1}) indicating the breakdown of urethane linkages. Since the peaks associated with hydroxyl groups also appear around this wavenumber, only small decrease in the peak intensity can be attributed to the formation of alcohols. Furthermore, the C═O stretching peak decreased in intensity, reflecting the conversion of urethane groups into urea derivatives. It was also noticed that there is a substantial decrease in C–N stretching and N–H bending vibrations after the amine treatment (orange line in Fig. 2b). Aminolysis transforms the urethane groups into urea deriva-

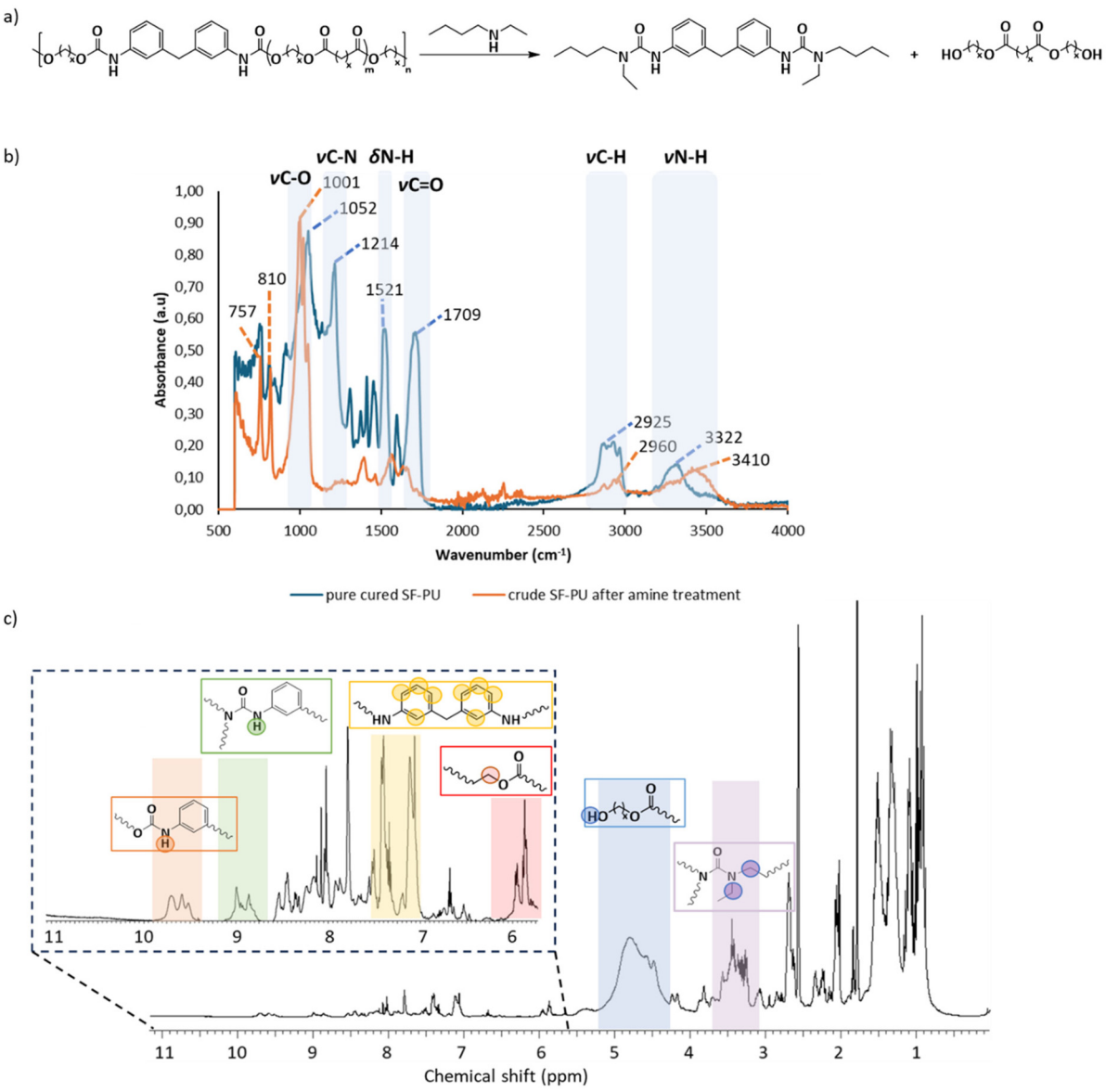

Fig. 2 (a) Chemical reaction scheme of aromatic polyester polyurethane (PU) with *N*-ethyl *N*-butyl amine (EBA); (b) FTIR spectra of the aromatic polyester polyurethane (PU) adhesive before and after EBA treatment; (c) NMR spectrum of the aromatic polyester polyurethane (PU) adhesive after EBA treatment.

tives and alcohols. The C–N bonds in the newly formed urea derivatives have different vibrational characteristics compared to those in the original urethane groups, which can result in a decrease in the C–N bending peak associated with the urethane linkages. Similarly, the newly formed urea groups can engage in different hydrogen bonding patterns compared to the urethane groups. The bending vibrations of the newly formed urea N–H bonds might not fully compensate for the loss of the original urethane N–H bonds, leading to an overall decrease in the N–H bending peak intensity. These spectral changes collectively confirm the aminolysis of polyurethane, where the original urethane bonds are cleaved, resulting in the formation of urea derivatives and alcohols.

Fig. 2c shows the NMR spectrum of the PU adhesive after the amine treatment. Aromatic protons are clearly observed between 6.5–8 ppm (yellow region), indicating that aromatic isocyanate was used in the PU adhesive formulation. In the spectrum, the proton peaks resonating around 10 ppm are observed, which corresponds to (CO)NH of urethane groups. This might be due to incomplete aminolysis of polyurethane, which is not the target of delamination and deinking in which merely a release of ink and layers is desired rather than producing monomers. Thus, oligomerization is a reasonable strategy. Upon aminolysis, urea derivatives and alcohols start to form. Substituted urea compounds generally appears in the aromatic protons region (between 6.5–8 ppm). The exact chemical shift of the N–H protons can be affected by electron-donating or electron-withdrawing groups attached to the urea nitrogen or carbonyl. In the PU adhesive, since the urea group is attached to an aromatic ring, there may be observable coupling between the urea N–H protons and the aromatic protons. This causes slight splitting or shifts in the urea peak, which appears around 9 ppm (green region). In addition the urea N–H peak appears to be broad. This might be due to hydrogen bonding or interactions with other groups in the molecule. Since the urea formed during aminolysis is also substituted with the amine used, the protons attached to the nitrogen of urea are detected between 3–4 ppm in multiples. Besides urea, alcohol is also formed during PU aminolysis. The broad peak appearing around 5 ppm (blue region) is assigned to the hydroxyl (OH) proton peak of the formed alcohol. Generally, polyols with multiple hydroxyl groups show multiple signals or a broad peak in this region due to hydrogen bonding. As it was deduced from the FTIR measurements that the PU adhesive is containing polyester based polyol, the protons attached to the ester band appears around 6 ppm in multiples in the NMR spectrum (red region). These changes in the NMR spectrum confirm the PU aminolysis and the formation of polyol, providing insights into the chemical transformation that has occurred. Regarding the recovery of aminolysis products, polyurea is expected to have low purity due to the presence of residual unreacted PU fragments. Therefore, recovering polyols at high purity after the aminolysis process is considered more promising. Once the polyurea fraction is removed by precipitation, the aminolysis medium is acidified to remove aromatic amines. This step leaves the liquid phase enriched primarily with polyols, which can then be recovered *via* liquid–liquid extraction or distillation.[65]

3.3. Influence of process parameters and medium composition on deinking efficiency

In addition to selecting amines with the right properties, deinking efficiency of plastic films can be further improved through optimization of process parameters such as temperature, solid-to-liquid (S/L) ratio, and particle size. Furthermore, given the fact that delamination/deinking occurs through aminolysis, the incorporation of chemical reagents alongside amines helps to boost the delamination and deinking efficiency. For example, apolar solvents can enhance the swelling of polymer layers, thereby facilitating the aminolysis of ink and adhesive components. Use of catalyst *e.g.* KOH would increase the efficiency of aminolysis. By combining these two strategies, deinking performance can be significantly improved. The following subsections will explore these approaches in detail, focusing on the influence of process parameters and reagent additions on the overall deinking efficiency of plastic materials.

3.3.1. Analyzing the effect of process conditions on deinking efficiency. To investigate the effect of process parameters on the deinking efficiency of plastic films, a kinetic study was performed on the violet colored PET/PE multilayer sample (sample 7 in Table 2) based on the DoE specified in Table 4. In the DoE, temperature, S/L ratio and particle size were considered, and the limits of each parameter were determined through screening tests. As the delamination time varies based on the experimental conditions, the maximum temperature was set at 65 °C to limit the curling of plastic film during treatment. The S/L ratio was tested in the range of 1% to 5%. While increased friction between plastic films at higher S/L ratios can promote delamination, 5% was set as the upper limit to prevent low stirring efficiency during the process and also to stay below the max concentration of reaction products. After conducting the set of experiments based on the DoE, the delamination % in *N*-ethyl *N*-butyl amine (EBA) after 90 minutes of reaction time was taken as a reference for each experimental condition to investigate the effect of process parameters on the delamination rate. The delamination% was calculated based on the initial amount of adhesive present at the start of the aminolysis reaction in each experiment as given in eqn (3) and (4). The corresponding delamination % for each kinetic test is shown in Fig. 3.

According to the experimental results, the delamination % was obtained under the conditions of Experiment 2 shown as red dots in Fig. 3 (at 57 °C, 1.2 cm particle size and 0.02 g mL^{-1} S/L ratio). On the other hand, the lowest delamination % was observed under the conditions of Experiment 7 shown as turquoise right-pointing triangle in Fig. 3 (at 33 °C, 3.3 cm particle size and 0.04 g mL^{-1} S/L ratio). In general, lower particle size and S/L ratio, and higher temperature resulted in higher reaction rate. However, as seen in Fig. 3, the lowest delamination % was not obtained at the lowest value of each parameter. For example, under the conditions of experiment 11, delamination % is more than three times higher than that achieved in experiment 10, despite the latter being conducted at a

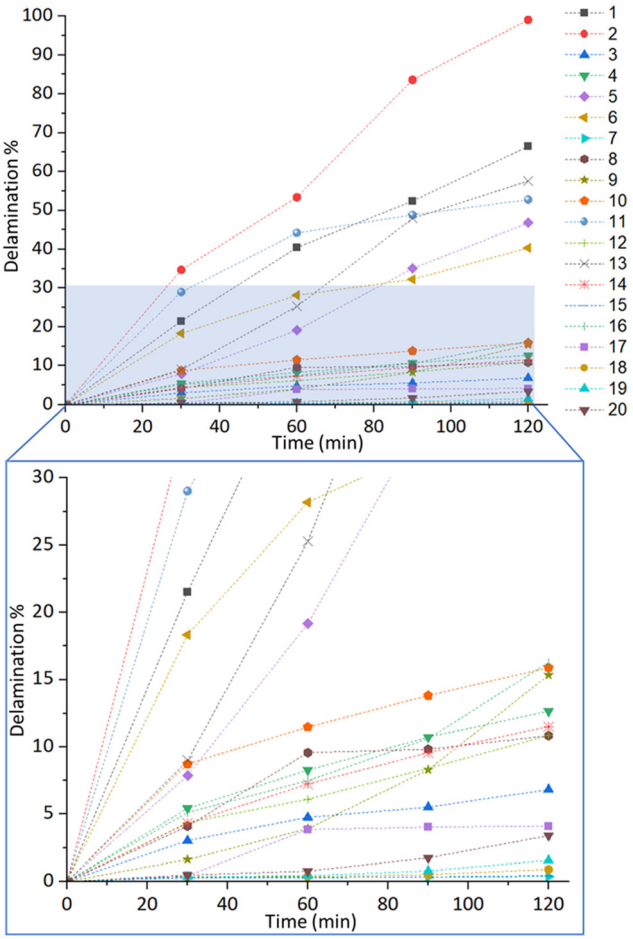

Fig. 3 Experimental kinetic data of delamination of the violet colored PET/PE multilayer sample (sample 7) through selective aminolysis of the adhesive in *N*-ethyl *N*-butyl amine (EBA) during 120 minutes. Detailed experimental data points are given in the SI, Table S2. The data points are connected with dashed lines for easier visualization. The standard deviation of delamination %, based on the 6 center points of DoE, is 5.97%.

higher temperature. This is due to the interaction between the experimental parameters which impacts the delamination rate. Therefore, the relationship between experimental parameters was described through Response Surface Methodology (RSM), as given in eqn (11) where $X1$, $X2$ and $X3$ refer to the coded values of temperature, particle size and S/L ratio, respectively. ε represents the model error, calculated as twice the residual standard error (5.75%), resulting in an estimated error of 11.5% at a 95% confidence interval.

$$\begin{aligned} Y_{\text{Delamination \%}} &= 2.9 + 1.4 \times X1 - 15.5 \times X2 - 7.7 \times X3 \\ &\quad + 2.9 \times X1^2 + 9.2 \times X2^2 + 9.2 \times X3^2 \\ &\quad + 2.5 \times X1 \times X2 + 3.6 \times X2 \times X3 \mp \varepsilon \end{aligned} \tag{11}$$

Using the quadratic equation and coefficients, it is possible to determine which parameter or interaction between parameters has the most pronounced effect on increasing delamination %. For example, among all the process variables, particle size ($X2$) makes the highest negative contribution (with a coefficient value 15.5), followed by S/L ratio ($X3$) for obtaining a higher delamination %. Similarly, in terms of interaction of the parameters, particle size and S/L ratio interaction plays a crucial role on increasing the delamination yield. The relationship between the experimental parameters and its effect on the delamination yield is visualized through the surface plots given in Fig. 4.

Fig. 4a shows that smaller particle size significantly enhance the delamination yield, even at lower temperatures. As the delamination rate was influenced by particle size, it suggests that lateral diffusion of the amine through the sides of the multilayer film can also play a significant role. In our research on the delamination and deinking of plastic films using carboxylic acids, there were indications that frontal diffusion of the acid was potentially more profound.[66] This may be attributed to the lower polarity of amines compared to short-chain carboxylic acids, which enhances polymer swelling and, in turn, increases the potential for lateral diffusion. The greater impact of reduced particle size on delamination yield,

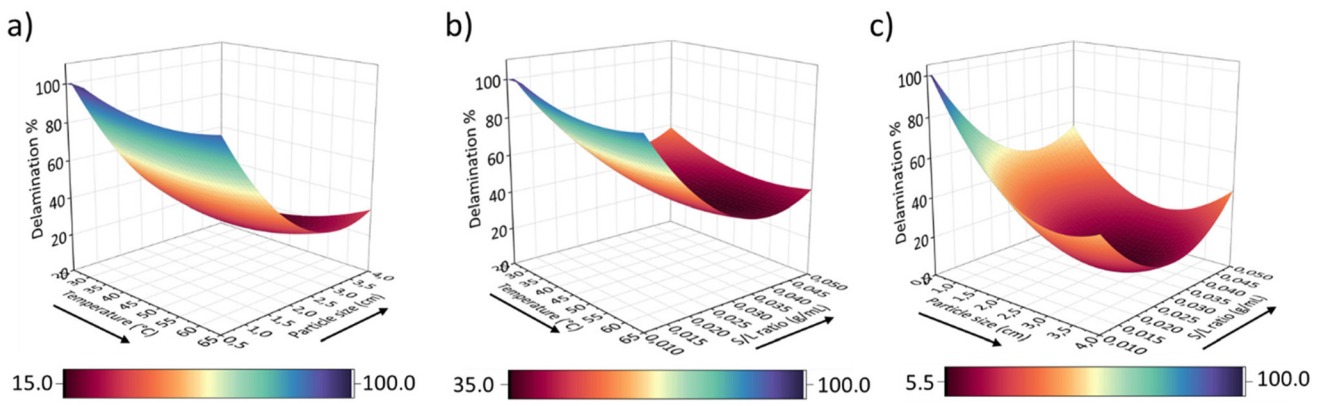

Fig. 4 Response surfaces of the delamination % as a function of (a) temperature (°C) and particle size (cm); (b) temperature (°C) and S/L ratio (g mL^{-1}); (c) particle size (cm) and S/L ratio (g mL^{-1}) for delamination of sample 7 through selective aminolysis of the PU adhesive layer. Delamination percentages exceeding 100% fall within the experimental error margin of the RSM model and are normalized to 100%.

compared to temperature increase, may be attributed to the relatively low temperature range used in the experiments to prevent curling or deformation of the polymer layers. During screening experiments, it was noted that the delamination rate significantly increases at temperatures above 70 °C; therefore, at lower temperatures, the increase in aminolysis rate is more restricted. This effect is also evident in the effect of interaction of temperature and S/L ratio on the delamination yield as shown in Fig. 4b. A decrease in the solid-to-liquid (S/L) ratio was found to have a more pronounced effect on improving the delamination yield. This is likely due to the relatively slow aminolysis rate of the adhesive. A reaction time of 90 minutes was chosen as a reference point in the construction of the quadratic model to more effectively capture the interactions among the process parameters. Within this time frame, the aminolysis of a smaller quantity of adhesive which corresponds to a lower S/L ratio, is more likely to reach completion than in experiments using a higher adhesive load. However, for large-scale delamination applications, a higher S/L ratio may still be considered to enhance the economic viability of the process, provided that the interaction time between the amine and plastic films is extended accordingly. As shown in Fig. 4c, combination of smaller particle size and lower S/L ratio resulted in increase in the delamination yield due to enhanced mass transfer between the solid film and the liquid phase. Based on all these interactions between the experimental parameters (temperature, S/L ratio, and particle size), optimal delamination conditions (from rate perspective) using EBA were determined as 65 °C, with 0.5 cm particle size and an S/L ratio of 0.01 g mL^{-1} for the violet colored PET/PE multilayer sample (sample 7).

3.3.2. Addition of chemical reagents

3.3.2.1. Improving delamination efficiency by swelling of the polymer layers. To improve delamination and deinking rates with amines, polymer swelling is used to facilitate diffusion. The swelling solvent must have high affinity for the polymer, but excessive affinity can dissolve the polymer rather than merely swell it. Additionally, the chosen solvent must not react with the amine. Taking these factors into account, various co-solvents were tested in combination with *N*-ethyl *N*-butyl amine (EBA), as shown in Fig. 5. Based on the Hansen Solubility Parameters (HSP), cyclohexane was tested at different volume ratios with EBA. The addition of cyclohexane had little impact on the deinking of UV-based inks but improved the delamination of multilayer samples. This is because the removal of UV-based inks primarily depends on the medium's chemical activity to break the crosslinking. In contrast, the delamination of multilayer films requires both the chemical activity of the medium and the swelling of the polymer layers to achieve effective separation. This effect was more pronounced on the pink OPP/PE multilayer sample. Due to the apolar nature of its constituent polymer layers, higher swelling in cyclohexane is expected compared to the PET/Al/PE multilayer sample, where the polar and metallic layers can reduce the solvent's effectiveness. Regarding the volume ratio of cyclohexane to EBA, increasing the cyclohexane content from 25% to 50% in the cyclohexane/EBA mixture resulted in a visually observed decrease in deinking efficiency for the black PET/Al/PE multilayer sample, while no significant change was observed for the pink OPP/PE multilayer sample. However, when the cyclohexane volume was further increased to 75%, both samples showed a decrease in deinking and delamination efficiency, based on visual observations. This suggests that an optimal balance between the swelling effect and the chemical activity of the amine is required for effective deinking and delamination.

Furthermore, the addition of more polar solvents such as ethanol and butanol to EBA at 25% was also tested, as shown in Fig. 5b. Compared to the cyclohexane addition, these polar solvents had a higher impact on the deinking and delamination of the black PET/Al/PE multilayer sample, likely due to the polar nature of the constituent polymer layer. Interestingly, the addition of polar solvents also improved the deinking of UV-based films. Similar to the results of cyclohexane, when butanol was used instead of ethanol, delamination and deinking were also successfully achieved for the pink OPP/PE multilayer sample. This also highlights the positive impact of using a lower polarity solvent for the delamination of multilayer samples composed primarily of apolar polymers. One hypothesis might be that this would swell the adhesive layer, allowing faster lateral diffusion of the amines, but this should be prone to further research. Interestingly, deinking of UV-based printed (low migration, LM) OPP film was lower in butanol compared to ethanol. This may be due to the higher polarity of ethanol, which enhances its ability to interact with the polar acrylic UV-based inks more effectively compared to butanol. Overall, the use of chemical reagents in combination with amines positively impacts the deinking and delamination efficiency of flexible plastic films, with the effect varying depending on the composition of the films.

3.3.2.2. Improving delamination efficiency by addition of a catalyst. The use of a strong base, such as potassium hydroxide (KOH), in combination with EBA was also evaluated, as shown in Fig. 5. The use of strong bases in aminolysis enhances both the reaction yield and the reaction rate.[67] While this approach achieved complete deinking and delamination for UV-printed films and the black PET/Al/PE multilayer sample, it had no noticeable effect on the pink OPP/PE multilayer. As discussed in the previous section, this could be attributed to the increased polarity of the medium. Increase in the deinking efficiency of other samples by addition of KOH would be due to the enhanced basicity of the reaction medium, which facilitates the breakdown of cross-linked ink networks, thereby promoting more effective ink removal and interlayer separation. However, this high reactivity came at a cost: undesired side reactions were observed, especially with sensitive layers such as polyethylene terephthalate (PET) and aluminum, resulting in signs of polymer degradation and structural compromise. To mitigate these adverse effects, a potential strategy would be the addition of a catalytic amount of base rather than using a high-concentration alkaline solution. This can retain the reactivity needed to facilitate delamination and deinking, while

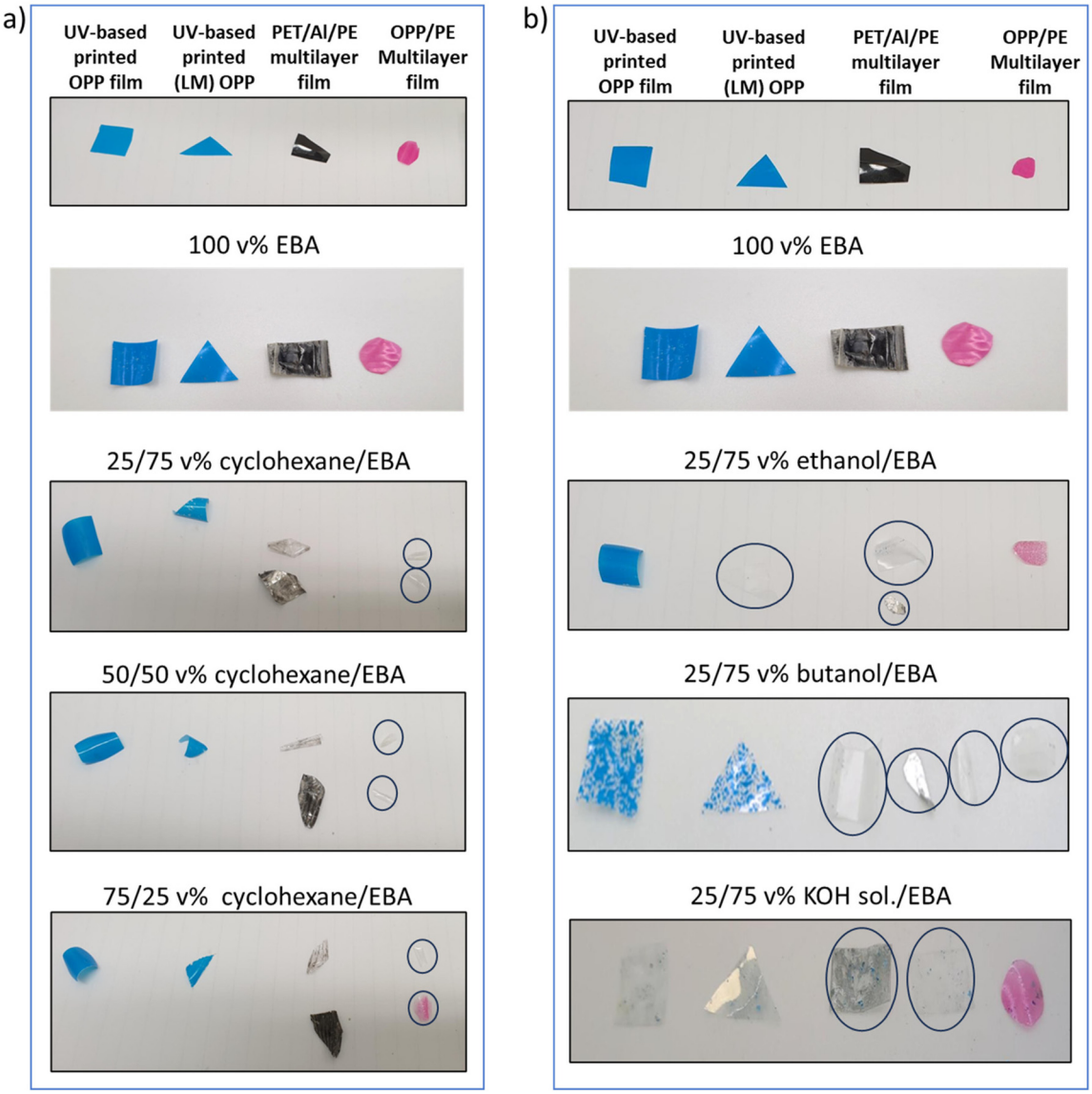

Fig. 5 Deinking and delamination of 4 different plastic films (a) in cyclohexane/*N*-ethyl *N*-butyl amine (EBA) mixture at different volume ratios; (b) in ethanol/EBA, butanol/EBA and KOH solution/EBA mixtures at 25/75 v% ratio after 4 h contact at 60 °C. Hourly visual progression of deinking and delamination of these samples in each medium is given in Fig. S5.

minimizing damage to the plastic and metallic layers. Ultimately, the careful selection and dosage of chemical reagents such as alkaline agents, solvents, or catalysts is essential to balance process efficiency with the preservation of material integrity. Tailoring the chemical environment to the specific composition of the plastic films ensures optimal performance of the delamination process without compromising recyclate quality.

4. Conclusion

Delamination and deinking of plastic packaging is a key process in the circular economy of plastics. In this study, selective aminolysis of adhesive and ink binders is proposed as a novel approach towards simultaneous deinking and delamination of monolayer and multilayer plastic films. In general, amines, potentially with additions of some solvent or catalyst are able to delaminate and deink a wide array of printed multilayer flexible packaging.

Our study shows that it would be beneficial to align amine type, depending on the plastic film structure if possible, maybe in future, based on advanced sorting. Regarding sample composition, multilayer films printed with UV-cured inks exhibited significantly lower deinking efficiency ($p < 0.05$) compared to other samples, with values below 10% for most amines. This is likely due to the high chemical resistance and crosslinked structure of UV-cured inks. Yet, primary amines

and diamines were effectively to deink multilayer films printed with UV-based inks. To map the effect of amine type, a quadratic model was developed that incorporated key physicochemical properties of amines, including boiling point, pK_b value, log *P*, molecular weight (MW), heat capacity, dipole moment, polar surface area, dipole polarizability, and molar volume. Among these properties, boiling point, heat capacity, dipole moment and polar surface area are found to be the most relevant properties in the model. For most of the samples, higher boiling point, in our case linked to apolarity, and polar surface area of the amine correlated with higher deinking efficiency, while higher heat capacity and dipole moment of amines resulted in lower deinking efficiency. Based on the coefficients of each amine property given in the quadratic equations, the dipole moment and polar surface area (PSA) showed the highest contribution to deinking efficiency. In a case study system with ethylbutylamine (EBA), the formation of polyols and urea derivatives confirmed *via* FTIR and NMR analyses that the mechanism is at least to a certain extent PU aminolysis, combined of course with the diffusion effects.

Key experimental parameters affecting the delamination and deinking process such as temperature, plastic flake size and solid/liquid ratio were investigated through a design of experiment. Based on the results from the RSM, the optimal conditions for achieving the highest delamination percentage of the violet PET/PE multilayer film (sample 7) using EBA were identified as 65 °C, a particle size of 0.5 cm, and an S/L ratio of 0.01 g mL^{-1}. Furthermore, it was demonstrated that addition of chemical reagents to amines such as solvents to enhance polymer swelling and catalysts *e.g.* KOH to accelerate aminolysis can have a positive effect on the effectiveness of the delamination and deinking, but impact varies with film composition and film quality needs to be considered.

As next steps, optimizing delamination conditions for different type of packaging, recovering the deinking medium, and validating the model with more plastics and amines will be essential. Future research should also focus on the safe handling of amines, considering their odor and potential ecotoxicity, to ensure environmental safety and feasibility, as well as on comprehensive economic feasibility studies for the industrial implementation of the process.

Conflicts of interest

There are no conflicts to declare.

Data availability

The data supporting this article have been included as part of the supplementary information (SI). Supplementary information is available. See DOI: https://doi.org/10.1039/d5gc02667a.

Acknowledgements

We thank Siegwerk Druckfarben AG & Co KGaA for providing the multilayer samples. This work was financially supported by the European Union's Horizon 2020 research and innovation program through the CIRCULAR FoodPack project under Grant Agreement number 101003806. This work was also performed in the framework of the CORNET project DEBOND (HBC.2022.0245 "DEBOND: Advancing recycling of multilayer plastics and textiles using an integrated approach for debonding on demand technology"), with the financial support of VLAIO (Flemish Agency for Innovation and Entrepreneurship). We would like to thank the Special Research Fund of Ghent University (BOF) (grant-code BOF.PDO.2024.0013.01) for the financial support.

References

1 European Commission, European Green Deal: Putting an end to wasteful packaging, boosting reuse and recycling [Internet], 2022 [cited 2023 Nov 7]. Available from: https://ec.europa.eu/commission/presscorner/detail/en/ip_22_7155.
2 OECD, Plastic pollution is growing relentlessly as waste management and recycling fall short, says OECD [Internet], 2022 [cited 2024 Aug 11]. Available from: https://www.oecd.org/en/about/news/press-releases/2022/02/plastic-pollution-is-growing-relentlessly-as-waste-management-and-recycling-fall-short.html#:~:text=22%2F02%2F2022%20%2D%20The,to%20a%20new%20OECD%20report.
3 A. Ogrinz, M. Pohl and B. Welling, Launching the circular economy in the chemical industry [Internet], 2022 [cited 2025 Aug 6]. Available from: https://www.chemiehoch3.de/fileadmin/user_upload/Chemie3_Guide_to_Circular_Economy.pdf.
4 Cefic, Getting started with the circular economy [Internet], 2024 [cited 2025 Aug 5]. Available from: https://cefic.org/case-study/getting-started-with-the-circular-economy/#:~:text=28%20November%202024,sustainability%20in%20the%20chemical%20industry.
5 Plastics Europe, The circular economy for plastics: A European overview [Internet], 2022 [cited 2025 Aug 5]. Available from: https://plasticseurope.org/wp-content/uploads/2022/06/PlasticsEurope-CircularityReport-2022_2804-Light.pdf.
6 R. Höfer, History of the Sustainability Concept – Renaissance of Renewable Resources, in *Sustainable Solutions for Modern Economies*, Royal Soc. of Chemistry, Cambridge, 1st edn, 2009.
7 BASF, Circular Economy [Internet], 2025 [cited 2025 Aug 5]. Available from: https://www.basf.com/global/en/who-we-are/sustainability/our-contributions-to-enabling-the-green-transformation/circular-economy.
8 J. Wang, The Transformation of China's Chemical Industry: Analysis of the Causes and Countermeasures

from the Perspective of Circular Economy. Advances in Economics, *Manage. Pol. Sci.*, 2023, **21**(1), 191–202.
9 K. Pyzyk, Henkel boosts recycled content in plastic packaging, PackagingDive [Internet], 2025 [cited 2025 Aug 5]; Available from: https://www.packagingdive.com/news/henkel-2024-sustainability-pcr-packaging/742766/.
10 Henkel, Henkel relaunches its bonding and sealing portfolio with recycled cartridges across Europe [Internet], Düsseldorf, 2023 [cited 2025 Aug 5]. Available from: https://www.henkel.com/press-and-media/press-releases-and-kits/2023-11-15-henkel-relaunches-its-bonding-and-sealing-portfolio-with-recycled-cartridges-across-europe-1899980.
11 Evonik. Product stewardship [Internet], 2023 [cited 2025 Aug 5]. Available from: Product Stewardship_EN_2023_ESHQ_TS (1).pdf.
12 J. N. Hahladakis, C. A. Velis, R. Weber, E. Iacovidou and P. Purnell, An overview of chemical additives present in plastics: Migration, release, fate and environmental impact during their use, disposal and recycling, *J. Hazard. Mater.*, 2018, **344**, 179–199.
13 O. Horodytska, F. J. Valdés and A. Fullana, Plastic flexible films waste management – A state of art review, *Waste Manage.*, 2018, **77**, 413–425.
14 J. Sutter, V. Dudler and R. Meuwly, Printing inks for food packaging composition and properties of printing inks [Internet], ILSI Europe Report Series, 2011 [cited 2021 Nov 30], 1–32 p. Available from: https://ilsi.eu/publication/packaging-materials-8-printing-inks-for-food-packaging-composition-and-properties-of-printing-inks/.
15 F. Awaja, M. Gilbert, G. Kelly, B. Fox and P. J. Pigram, Adhesion of polymers, *Prog. Polym. Sci.*, 2009, **34**, 948–968.
16 Flexible Packaging, Resins Key to Packaging Ink Performance [Internet], 2019 [cited 2020 Sep 15]. Available from: https://www.flexpackmag.com/articles/90163-resins-key-to-packaging-ink-performance.
17 C. Domeño, M. Aznar, C. Nerín, F. Isella, M. Fedeli and O. Bosetti, Safety by design of printed multilayer materials intended for food packaging, *Food Addit. Contam., Part A: Chem., Anal., Control, Exposure Risk Assess.*, 2017, **34**(7), 1239–1250.
18 K. Kaiser, M. Schmid and M. Schlummer, Recycling of polymer-based multilayer packaging: A review, *Recycling*, 2018, **3**, 1–26.
19 Bobst, Transparent MDO PE solutions as an alternative to Metallized Polyester [Internet], 2021 [cited 2023 Nov 10]. Available from: https://www.bobst.com/usen/news/detail/article/1611838980-transparent-mdo-pe-solutions-as-an-alternative-to-metallized-polyester/.
20 M. Roosen, L. Harinck, S. Ügdüler, T. De Somer, A. G. Hucks, T. G. A. Belé, *et al.*, Deodorization of post-consumer plastic waste fractions: A comparison of different washing media, *Sci. Total Environ.*, 2022, **812**, 152467.
21 H. Gecol, J. F. Scamehorn, S. D. Christian and F. E. Riddell, Use of surfactants to remove solvent-based inks from plastic films, *Colloid Polym. Sci.*, 2003, **281**(12), 1172–1177.
22 H. Gecol, J. F. Scamehorn, S. D. Christian, B. P. Grady and F. Riddell, Use of surfactants to remove water based inks from plastic films, *Colloids Surf., A*, 2001, **189**, 55–64.
23 H. Gecol, J. F. Scamehorn, S. D. Christian, B. P. Grady and F. E. Riddell, Deinking of water-based ink printing from plastic film using nonionic surfactants, *J. Surfactants Deterg.*, 2002, **5**(4), 363–374.
24 A. Chotipong, J. F. Scamehorn, T. Rirksomboon, S. Chavadej and P. Supaphol, Removal of solvent-based ink from printed surface of high-density polyethylene bottles by alkyltrimethylammonium bromides: Effects of pH, temperature, and salinity, *Colloids Surf., A*, 2007, **297**, 163–171.
25 A. Piolat, Method and apparatus for recycling printed plastic films. EU patent office, EP1419829A1, 2002.
26 Keycycle, CADEL Deinking is now KEYCYCLE Deinking [Internet], 2023 [cited 2024 Jan 15]. Available from: https://www.keycycle.at/en/keycycle-deinking/.
27 Sorema, Ink removal in plastics recycling plants [Internet], 2021 [cited 2025 Feb 13]. Available from: https://sorema.it/en/news-events/news/ink-removal-in-plastics-recycling-plants.
28 H. M. El Refay, N. Badawy, A. Hamada and E. S. Hassen, Separation of Some Anionic Dyes Using Reverse Micelles of CTAB and SDS as Efficient Surfactants Adsorbents from Aqueous Medium, *Int. J. Chem. Eng.*, 2022, **2022**, 1–16.
29 R. Höfer, Solvents and Green Solvents in Polymers and Industry—Devil or Savior?, in *Reference Module in Materials Science and Materials Engineering*, Elsevier, Düsseldorf, 2024.
30 RPC bpi group, Norec [Internet], 2018 [cited 2021 May 28]. Available from: https://www.rpc-bebo.com/assets/sustainability-files/responsibility-report.pdf.
31 A. Gürses, M. Açıkyıldız, K. Güneş and M. S. Gürses, Dyes and Pigments: Their Structure and Properties, in *Dyes and Pigments*, Springer, Cham, 2016, pp. 13–29.
32 S. Ügdüler, T. Van Laere, T. De Somer, S. Gusev, K. M. Van Geem, A. Kulawig, *et al.*, Understanding the complexity of deinking plastic waste: An assessment of the efficiency of different treatments to remove ink resins from printed plastic film, *J. Hazard. Mater.*, 2023, **452**, 131239–131255.
33 C. J. Lynch and E. B. Nauman, Polymer recycling by selective dissolution, *US*, US5278282A, 1994.
34 R. D. Thome, S. Kraus and J. Schubert, Process for treating or working up composite and plastic materials, *EU*, EP0644230A1, 1993.
35 R. Kippenhahn, U. Knauf, T. Luck, A. Mäurer, M. Schlummer and G. Wolz, Method for separating and recovering target polymers and their additives from a material containing polymers, *EU*, EP1311599A1, 2003.
36 A. Mäurer and M. Schlummer, Good as new. Recycling plastics from WEEE and packaging wastes, *Waste Manage. World*, 2004, **4**, 33–34.
37 W. Adam, Dissolution process, UK, Worn Again Tech Ltd, GB2560726A, 2017.
38 A. Walker, Process for extracting polyester from an article, Withers & Rogers LLP, WO2014045062A1, 2013.

39 CreaSolv, The CreaSolv® Process [Internet], 2018 [cited 2025 Aug 5]. Available from: https://www.creasolv.de/en/the-process.html.
40 Packaging Europe, APK scales recycling technology for post-consumer waste [Internet], 2024 [cited 2025 Aug 11]. Available from: https://packagingeurope.com/news/apk-scales-recycling-technology-for-post-consumer-waste/11536.article.
41 PureCycle. PureCycle Technologies [Internet]. [cited 2021 May 28]. Available from: https://www.purecycle.com/our-process.
42 K. L. Sánchez-Rivera, P. Zhou, M. S. Kim, L. D. González Chávez, S. Grey, K. Nelson, *et al.*, Reducing Antisolvent Use in the STRAP Process by Enabling a Temperature–Controlled Polymer Dissolution and Precipitation for the Recycling of Multilayer Plastic Films, *ChemSusChem*, 2021, **14**(19), 4317–4329.
43 R. Kol, T. De Somer, D. R. D'hooge, F. Knappich, K. Ragaert, D. S. Achilias, *et al.*, State-Of-The-Art Quantification of Polymer Solution Viscosity for Plastic Waste Recycling, *ChemSusChem*, 2021, **14**(19), 4071–4102.
44 A. C. Massura, E. A. Marçal De Souza and G. B. Crochemore, Process for separation of multilayered films used for packagings, WO2003104315A1, 2002..
45 J. Kersting, Process for separating aluminum foils from plastic foils, in particular PE foils, *Germany*, DE4137895C2, 2000.
46 C. K. Huang and C. H. Shao, Separating method for recycling foil-laminated material, *US*, US20040129372A1, 2002.
47 D. Xianghui, Plastic-aluminum separating agent and plastic-aluminum separating method, *China*, CN100535039C, 2007.
48 S. Ügdüler, T. De Somer, K. M. Van Geem, M. Roosen, A. Kulawig, R. Leineweber, *et al.*, Towards a better understanding of delamination of multilayer flexible packaging films by carboxylic acids, *ChemSusChem*, **2021**, 4198–4213.
49 G. O'Rourke, M. Houbrechts, M. Nees, M. Roosen, S. De Meester and D. De Vos, Delamination of polyamide/polyolefin multilayer films by selective glycolysis of polyurethane adhesive, *Green Chem.*, 2022, 6867–6878.
50 M. Lindner, N. Rodler, M. Jesdinszki, M. Schmid and S. Sängerlaub, Surface energy of corona treated PP, PE and PET films, its alteration as function of storage time and the effect of various corona dosages on their bond strength after lamination, *J. Appl. Polym. Sci.*, 2018, **135**, 1–9.
51 S. A. Syed Ali, I. M. S. K. Ilankoon, L. Zhang and J. Tan, Understanding de-inking in packaging plastic recycling: Bridging the gap in resource conservation and establishing average hazard quotient, *J. Hazard. Mater.*, 2024, **479**, 135554.
52 A. Mukhopadhyay, Process of de-lamination of multi-layer laminated packaging industrial refuse, *US*, US20040054018A1, 2001.
53 K. M. Patel, M. M. Patel and M. H. Vaviya, Process for recovering low-density polyethylene from flexible packaging material. CHAKRAVARTHY, Kalyan, WO2015159301A3, 2016.
54 H. Hanel and K. Wohnig, Method for plastic pre-treatment and solvent-based plastic recycling. APK AG, WO2022029318A1, 2021.
55 C. Samorì, W. Pitacco, M. Vagnoni, E. Catelli, T. Colloricchio, C. Gualandi, *et al.*, Recycling of multilayer packaging waste with sustainable solvents, *Resour., Conserv. Recycl.*, 2023, **190**, 106832.
56 T. Narr and W. Giefing, Recycling process treating wastes, plastic mixtures and plastic composites, Kerec Kunststoff und Elektroni, DE19651571A1, 1996.
57 I. Eide-Haugmo, O. G. Brakstad, K. A. Hoff, K. R. Sørheim, E. F. da Silva and H. F. Svendsen, Environmental impact of amines, *Energy Procedia*, 2009, **1**(1), 1297–1304.
58 J. Guo, C. Luo, C. Wittkowski, I. Fehr, Z. Chong, M. Kitzberger, *et al.*, Screening the Impact of Surfactants and Reaction Conditions on the De-Inkability of Different Printing Ink Systems for Plastic Packaging, *Polymers*, 2023, **15**(9), 2220.
59 Siegwerk Druckfarben AG & Co. KGaA. Declaration on the use of Low molecular weight photoinitiators in standard UV printing inks and varnishes not intended for "NPH" (nutrition, pharma and hygiene) applications [Internet], 2023 [cited 2025 Apr 23]. Available from: https://www.siegwerk.com/fileadmin/Data/Documents/ProductSafety/en/Low_molecular_weight_PI_for_non-NPH_applications_3.0_EN.pdf.
60 BASF. Inks for flexible packaging [Internet], 2014 [cited 2025 Apr 23]. Available from: https://www.basf.com/us/en/products/General-Business-Topics/dispersions/Industries/printing_packaging0/flexible_packaging/fp_inks.
61 Plastic Recycling Machine. PET bottle recycling [Internet], 2013 [cited 2020 Feb 18]. Available from: https://www.pet-bottlewashingline.com/pet-bottle-recycling/.
62 Evonik. Enabling circularity! TEGO® Res 1100 ensures faster and better deinking of plastic packaging waste – leading to high recyclate quality [Internet], 2025 [cited 2025 Aug 14]. Available from: https://www.evonik.com/en/news/news-stories/2025/enabling-circularity–tego–res-1100-ensures-faster-and-better-d.html.
63 Henkel AG & Co. KGaA. Debond-on-demand adhesives are unlocking progress toward a circular economy [Internet], 2025 [cited 2025 Aug 14]. Available from: https://www.henkel.com/our-businesses/adhesive-technologies/about-us/debond-on-demand-adhesives-are-unlocking-progress-toward-a-circular-economy-2065782.
64 Siegwerk. Siegwerk launches new generation of PUR inks to drive the future of gravure printing [Internet], 2016. [cited 2025 Aug 14]. Available from: https://www.siegwerk.com/en/news-media/press-releases/details/siegwerk-launches-new-generation-of-pur-inks-to-drive-the-future-of-gravure-printing.html.
65 M. Grdadolnik, B. Zdovc, A. Drinčić, O. C. Onder, P. Utroša, S. G. Ramos, *et al.*, Chemical Recycling of Flexible

Polyurethane Foams by Aminolysis to Recover High-Quality Polyols, *ACS Sustainable Chem. Eng.*, 2023, **11**(29), 10864–10873.

66 S. Ügdüler, T. De Somer, K. M. Van Geem, J. De Wilde, M. Roosen, B. Deprez, *et al.*, Analysis of the kinetics, energy balance and carbon footprint of the delamination of multilayer flexible packaging films via carboxylic acids, *Resour., Conserv. Recycl.*, 2022, **181**, 106256.

67 C. L. Chang and Y. K. Lin, Competition of aminolysis and alcoholysis in nucleophilic cleavage of a model compound for polysiloxane networks, *Polym. Degrad. Stab.*, 2005, **87**(1), 207–211.